



HAL
open science

Mouse Parthenogenetic Embryonic Stem Cells with Biparental-Like Expression of Imprinted Genes Generate Cortical-Like Neurons That Integrate into the Injured Adult Cerebral Cortex

Annie Varrault, Sigrid Eckardt, Benoît Girard, Anne Le Digarcher, Isabelle Sasseti, Céline Meusnier, Chantal Ripoll, Armen Badalyan, Federica Bertaso, K. John McLaughlin, et al.

► To cite this version:

Annie Varrault, Sigrid Eckardt, Benoît Girard, Anne Le Digarcher, Isabelle Sasseti, et al.. Mouse Parthenogenetic Embryonic Stem Cells with Biparental-Like Expression of Imprinted Genes Generate Cortical-Like Neurons That Integrate into the Injured Adult Cerebral Cortex. *STEM CELLS*, 2018, 36 (2), pp.192 - 205. 10.1002/stem.2721 . hal-01788655

HAL Id: hal-01788655

<https://hal.umontpellier.fr/hal-01788655v1>

Submitted on 9 Oct 2024

HAL is a multi-disciplinary open access archive for the deposit and dissemination of scientific research documents, whether they are published or not. The documents may come from teaching and research institutions in France or abroad, or from public or private research centers.

L'archive ouverte pluridisciplinaire **HAL**, est destinée au dépôt et à la diffusion de documents scientifiques de niveau recherche, publiés ou non, émanant des établissements d'enseignement et de recherche français ou étrangers, des laboratoires publics ou privés.



HHS Public Access

Author manuscript

Stem Cells. Author manuscript; available in PMC 2019 February 01.

Published in final edited form as:

Stem Cells. 2018 February ; 36(2): 192–205. doi:10.1002/stem.2721.

Mouse parthenogenetic embryonic stem cells with biparental-like expression of imprinted genes generate cortical-like neurons that integrate into the injured adult cerebral cortex

Annie Varrault^{1,*}, Sigrid Eckardt², Benoît Girard¹, Anne Le Digarcher¹, Isabelle Sassetti³, Céline Meusnier¹, Chantal Ripoll³, Armen Badalyan¹, Federica Bertaso¹, K. John McLaughlin², Laurent Journot¹, and Tristan Bouschet^{1,*}

¹Institut de Génomique Fonctionnelle, IGF, CNRS, INSERM, Univ. Montpellier, F-34094 Montpellier, France

²Research Institute at Nationwide Children's Hospital, Center for Molecular and Human Genetics, Columbus, OH, 43205, USA

³Institute for Neuroscience of Montpellier, Hôpital Saint Eloi, 34091 Montpellier cedex 5, France

Abstract

One strategy for stem cell-based therapy of the cerebral cortex involves the generation and transplantation of functional, histocompatible cortical-like neurons from embryonic stem cells (ESCs). Diploid parthenogenetic Pg-ESCs have recently emerged as a promising source of histocompatible ESC derivatives for organ regeneration but their utility for cerebral cortex therapy is unknown. A major concern with Pg-ESCs is genomic imprinting. In contrast with biparental Bp-ESCs derived from fertilized oocytes, Pg-ESCs harbor two maternal genomes but no sperm-derived genome. Pg-ESCs are therefore expected to have aberrant expression levels of maternally expressed (MEGs) and paternally expressed (PEGs) imprinted genes. Given the roles of imprinted genes in brain development, tissue homeostasis and cancer, their deregulation in Pg-ESCs might be incompatible with therapy. Here, we report that, unexpectedly, only one gene out of 7 MEGs and 12 PEGs was differentially expressed between Pg-ESCs and Bp-ESCs while 13 were differentially expressed between androgenetic Ag-ESCs and Bp-ESCs, indicating that Pg-ESCs but not Ag-ESCs, have a biparental-like imprinting compatible with therapy. In vitro, Pg-ESCs generated cortical-like progenitors and electrophysiologically active glutamatergic neurons that maintained the biparental-like expression levels for most imprinted genes. In vivo, Pg-ESCs participated to the cortical lineage in fetal chimeras. Finally, transplanted Pg-ESC derivatives integrated into the injured adult cortex and sent axonal projections in the host brain.

*Correspondence: Annie Varrault, Ph.D. and Tristan Bouschet, Ph.D. Institut de Génomique Fonctionnelle, CNRS UMR-5203, INSERM-U1191, Université de Montpellier, 141 rue de la Cardonille, F-34094, France. Telephone: +33(0)434 359 240, Fax: +33(0)467 542 432. Annie.Varrault@igf.cnrs.fr or Tristan.Bouschet@igf.cnrs.fr.

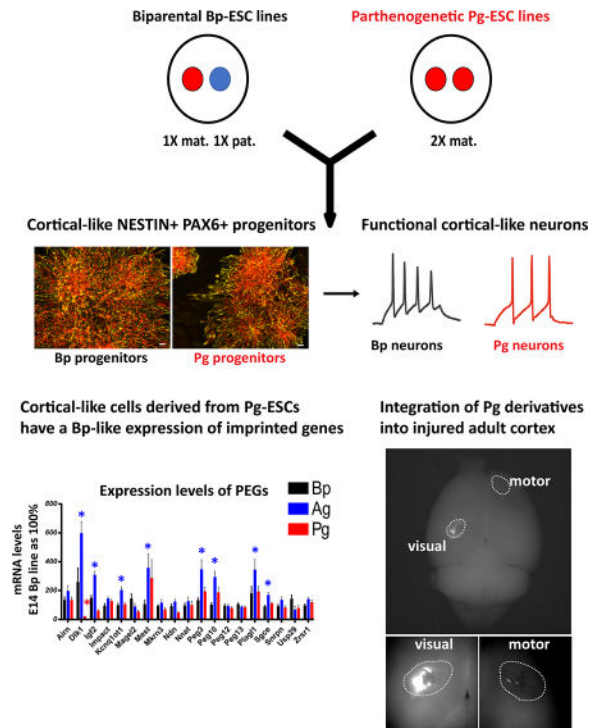
Conception and design: A.V., S.E., K.J.M., L.J. and T.B. Financial support: K.J.M. and L.J. Provision of study materials: A.V., S.E., K.J.M., L.J. and T.B. Collection and/or assembly of data: A.V., S.E., B.G., A.L.D., I.S., C.M., C.R., A.B., F.B., K.J.M., L.J. and T.B. Data analysis and interpretation: A.V., S.E., B.G., A.L.D., I.S., C.M., F.B., A.B. K.J.M., L.J. and T.B. Manuscript writing: A.V., S.E., K.J.M., L.J. and T.B. Final approval of manuscript: all authors.

Competing interests

No competing interests declared.

In conclusion, mouse Pg-ESCs generate functional cortical-like neurons with biparental-like imprinting and their derivatives properly integrate into both the embryonic cortex and the injured adult cortex. Collectively, our data support the utility of Pg-ESCs for cortical therapy.

Graphical abstract



Keywords

Embryonic stem cells; Neural differentiation; Cellular therapy; Cerebral cortex; Imprinting; Chimeric; Parthenogenesis; Stem cell transplantation

Introduction

The cerebral cortex is crucial for higher cognitive, sensory and motor functions. In the adult cortex, there is no neurogenesis to compensate for neuronal loss caused by disease or injury [1]. Cortical-like neurons produced from normal, biparental (Bp) pluripotent cells, including mouse and human embryonic stem cells (ESCs), are a promising source of cortical transplants [2–4]. However, a major hurdle remains graft rejection because the central nervous system is not devoid of immunological responses [5]. For example, neural progenitors transplanted into the spinal cord are rejected due to a poor match with the major histocompatibility complex (MHC) of the host [6]. The use of induced pluripotent stem cells is promising to improve histocompatibility [7] but reprogramming might transmute the cell genome and epigenome, resulting in an impaired safety [8].

One emerging alternative is to use parthenogenetic ESCs (Pg-ESCs). Pg-ESCs are derived from unfertilized eggs and they contain two maternal genomes and no paternal genome [9].

Pg-ESCs are frequently homozygous at MHC/HLA loci and can be therefore more easily selected for histocompatibility than normal biparental (Bp) ESC lines [7, 10, 11]. For example, a collection of human Pg-ESC lines established from 55 oocyte donors would perfectly match the three HLA loci for 80% of the Japanese population [12]. Furthermore, the neural derivatives of Pg-ESCs are more resistant to natural killer cells than Bp-ESC derivatives [13]. Mouse and human Pg-ESCs can be differentiated in vitro and in vivo into derivatives of all germ lineages [11, 14], including neural lineages [13, 15, 16]. Pg-ESCs have therefore emerged as a potent source of histocompatible cells for liver [17], heart [18], hematopoietic tissue [19], tendon [20] and the substantia nigra [16]. Finally, Pg-ESCs are a more accessible source with less ethical concerns than Bp blastocysts developed from sperm fertilized-eggs.

Two important issues need to be addressed when using Pg-ESCs for cortical therapy. The first issue, which concerns all tissues derived from Pg-ESCs, is about their parental imprinting. Imprinted expression of a small number of genes is required for proper embryonic development [21, 22] and tissue homeostasis by controlling tissue-resident stem cells [23]. Conversely, deregulation of imprinting triggers tumorigenesis in mouse [24] and abnormal levels of imprinted genes are frequently observed in human cancers [25]. Pg-ESCs are expected to display a drastic deregulation of imprinted genes, with high expressing maternally expressed genes (MEGs) and low expressing paternally expressed genes (PEGs) when compared to Bp-ESCs. Some studies have confirmed such expression bias for some imprinted genes while others have found that Pg-ESC imprinting is relatively similar to that of Bp-ESCs [18, 26–35]. Importantly, most of these studies were performed on few imprinted genes and/or only one Pg-ESC line. In addition, imprinting is developmental stage- and tissue-dependent [36] and these studies did not investigate PEGs and MEGs with ESC-specific expression patterns. In this context, using RNA-seq on hybrid ESC lines, we have recently established an extensive list of MEGs and PEGs specific to mouse Bp-ESCs [37].

The second issue is about the ability of Pg-ESCs to be differentiated into functional cortical-like cells. Pg-ESC derivatives populate the cortex of chimeras in vivo [38]. However, whether Pg-ESC derivatives display specific features of cortical cells such as a radial orientation and expression of cortical markers is unknown. Numerous imprinted genes are expressed in a parent-of-origin dependent manner in the developing cortex generated in vivo, or in vitro from ESCs [37]; and some of them, including *Cdkn1c* [39], *Plagl1* [40], *Dlk1* [41] and *Igf2* [42], are required for proper corticogenesis in the mouse. Humans suffering from imprinting disorders (including Angelman syndrome, Prader-Willi syndrome and transient neonatal diabetes mellitus) exhibit impaired corticogenesis [43–45]. Collectively, this suggests that Pg-ESCs might be not capable of undergoing normal corticogenesis because of aberrant expression levels of imprinted genes that are important for corticogenesis.

Here, we have first clarified the imprinting status of mouse Pg-ESCs by quantifying the expression levels of 26 imprinted genes, including 7 validated MEGs and 12 validated PEGs in ESCs [37], in three independent Pg-ESC lines, and in two normal Bp-ESC and two androgenetic Ag-ESC lines. Ag-ESCs have two paternal genomes and form tumors in chimeras [46]. Here, we confirm that Ag-ESC lines have low expressing MEGs and high

expressing PEGs [27, 34, 47]. Oppositely, we found that Pg-ESC imprinting was surprisingly biparental-like. Next, Pg-ESC lines were differentiated according to an established protocol of *in vitro* corticogenesis that reproduces the main features of *in vivo* corticogenesis [2], including the parent-of-origin dependent expression of imprinted genes [37]. We found that Pg-ESCs generated cortical-like progenitors and electrophysiologically active glutamatergic neurons. Importantly, cortical-like Pg derivatives maintained the biparental-like expression for most imprinted genes. Furthermore, Pg-ESC derivatives participated well to the cortical lineage in embryonic chimeras. Finally, transplanted Pg-ESC derivatives integrated into the injured adult cortex and sent axonal projections in the host brain.

In conclusion, Pg-ESCs generate functional cortical neurons with a biparental-like imprinting and Pg-ESC derivatives integrate properly into the mouse embryonic cortex and the injured adult cortex. Our study therefore gives support for the utility of Pg-ESC derivatives for future cellular therapies, including for neocortex repair.

Materials and Methods

ESC culture

The biparental (Bp) ESC lines were E14Tg2a –hereafter E14- [37], WT-B1 [19] and Tau-eGFP [48]; the Ag-ESC lines were AK2 [49] and AG-B6 [19]; the Pg-ESC lines were PG-BT6 [50] and PG-08-21 (both from Columbus, USA) and PR8 [49] (from Cambridge, UK). E14 was maintained on gelatin and the six other lines were propagated on mitomycin-treated MEFs in DMEM (Invitrogen) supplemented with 15% ESC-certified FBS (Invitrogen), 0.1mM non-essential amino acids (Invitrogen), 1mM sodium pyruvate (Invitrogen), 0.1mM β -mercaptoethanol (Sigma), 50U/ml penicillin/streptomycin and 10^3 U/ml LIF (Millipore) as described [37]. All ESC lines were regularly controlled to exclude the presence of mycoplasma using the Mycoalert kit (Lonza).

In vitro corticogenesis was performed as previously described [37, 51]. Before differentiation, all ESC lines were acclimated to the absence of feeders and grown on gelatin (as E14) for at least one passage. ESCs were plated at low density on gelatin-coated dishes or coverslips and cultured in DMEM/F12 supplemented with N2 supplement (Invitrogen) and cyclopamine (Merck) as described [37, 51]. ESCs were differentiated for 12 (d12) and 21 (d21) days except for patch-clamp recordings (four weeks).

Generation of fetal chimeras

Chimeras were generated using WT-B1, AG-B6 and PG-08-21 ESCs, which contain a beta-actin promoter with a CMV enhancer driving GFP expression (see supplementary information). ESCs were injected into C57BL/6J blastocysts followed by embryo transfer into pseudo pregnant CD-1 (Hsd:ICR (CD-1[®]); Harlan Laboratories) female mice [52]. Fetuses were recovered at E12.5 and chimeras identified using GFP fluorescence. These experiments were carried out in strict accordance with the recommendations in the Guide for the Care and Use of Laboratory Animals of the National Institutes of Health. The protocol

was approved by the Animal Care and Use Committee (IACUC) at the Research Institute at Nationwide Children's Hospital (Permit Number: # AR09-00051).

Grafting of ESC derivatives into the injured adult cortex

All grafting experiments were conducted in accordance with the European Communities Council Directive (2010/63/EU) and approved by the French Ministry for Agriculture (Permit Number: #10401). Four month-old adult C57BL/6 mice were anesthetized with ketamine and xylazine and parts of the left visual cortex and right motor cortex were aspirated. ~100,000 cells (in 1 μ l PBS with 0.6% glucose) derived from PG-08-021, Tau-GFP or WT-B1 ESCs differentiated for 13–16 days were injected into the lesion using a Hamilton pipette. Transplants were analyzed 15 to 18 days post-grafting. All mice (n=21) survived the transplantation procedure.

Immunostaining on in vitro and in vivo cortex

In vitro samples were processed as described [37, 51]. The brains of transplanted adult mice were first imaged using a Discovery.V12 stereomicroscope (Zeiss) to localize the presence of GFP⁺ grafts and then free-floating sections (100 μ m thick) were made. Cryosections (20 μ m thick) were made from the heads of fetal chimeras sacrificed at E12.5. A detailed protocol for immunostaining, including the list of antibodies, is provided in supplementary information. Each staining was performed at least on three different animals of each genotype and on at least three different in vitro cortex samples.

Analysis of the expression of imprinted genes and cell fate markers

RT-qPCRs were performed as described [37]. The expression levels of 34 imprinted genes and 25 markers of cell fate were normalized to the expression levels of three housekeeping genes using the qPCR primers listed in Table S1.

DNA methylation

Genomic DNAs (gDNAs) were prepared using the Purelink genomic DNA kit (Life Technologies). For methylation analysis by targeted bisulfite sequencing of specific loci, bisulfite conversion was performed using the EpiTech kit (Qiagen). PCR amplifications, cloning, and sequencing at the H19-DMR and IG-DMR were performed as described [37, 53]. For methylation analysis by M_{cr}BC, gDNAs were either left untreated or digested by M_{cr}BC and qPCR was performed as described above. For each DNA locus, the C_p values for digested and undigested DNAs were measured in triplicate. 2^{-C_p} values were obtained by normalizing using 3 genomic sequences resistant to M_{cr}BC digestion (*Col1a2*, *Col3a1*, and *Col9a2*). The % of DNA methylation at a given DNA locus was calculated as follows: % methylated DNA = 100 * (1 - (2^{-C_p} digested / 2^{-C_p} undigested)). Primers are listed in Table S1.

Patch-clamp recording

Whole-cell patch-clamp recording was performed at room temperature on cells with a typical cortical pyramidal morphology after 4 weeks of corticogenesis. Data were recorded using an Axopatch-200 amplifier (Molecular Devices, CA, USA), filtered with a HumBug

(Quest Scientific, Canada), digitized at 2 kHz (Digidata 1444A, Molecular Devices), and acquired using Clampex 10.2 software (Molecular Devices). Reagents are detailed in supplementary information.

Statistical analysis

Electrophysiological parameters were compared using an unpaired Student's t-test between Bp neurons and uniparental neurons ($p < 0.05$). Data are presented as mean + s.e.m. Mann-Whitney test was used for McrBC-based methylation assays, using GraphPad Prism. For RT-qPCR, a Mann-Whitney test was performed to determine p values that were then adjusted according to the Benjamini-Hochberg false discovery rate procedure. Values with an adjusted- $p < 0.05$ were considered as significantly different between two conditions.

Results

Pg-ESCs exhibit normal levels of pluripotency and proliferation markers

We first evaluated the stemness of Pg-ESCs by quantifying the expression of four pluripotency and proliferation markers in three independent mouse Pg-ESC lines from two different sources. As controls, two biparental Bp-ESC and two androgenetic Ag-ESC lines (from two sources as well) were included. More than 95% of Pg-ESCs were POU5F1⁺, as were Bp-ESCs and Ag-ESCs (Fig. S1A, C, E, and quantified in G). Only a subset of ESCs of each line were NANOG⁺, as described for Bp-ESCs maintained in similar culture conditions [54] (Fig. S1B, D, F). The average expression levels of *Pou5f1* and *Nanog* were similar in Pg-ESCs and Bp-ESCs (Fig. S1H, I), despite variability for *Nanog* between individual ESC lines (Fig. S2). The two proliferation markers *Mki67* and *Pcna* were also expressed at comparable levels (Figs. S1J, K and S2), in agreement with a previous study showing that duration of the cell cycle is similar in Pg-ESCs and Bp-ESCs [55]. Thus, undifferentiated Pg-ESCs exhibit proper expression of two pluripotency and two proliferation markers.

Pg-ESCs display a biparental-like expression of imprinted genes

To clarify the imprinting status of the three Pg-ESC lines, we quantified the expression levels of 26 imprinted genes that we have previously identified as MEGs (7 genes), PEGs (12 genes) or biallelically expressed (BA, 7 genes) in ESCs [37]. As controls, the two Bp-ESC and two Ag-ESC lines were also included. Because Pg-ESCs harbor two copies of maternal genome, they should have low expressing PEGs and high expressing MEGs. Surprisingly, we found that the expression levels of all 12 tested PEGs were not different between Pg-ESCs and Bp-ESCs and that *H19* was the only differentially expressed MEG (adjusted- $p < 0.05$) (Fig. 1A, B). Available published data show that biparental expression of at least a subset of imprinted genes is frequent in Pg-ESC lines ([18, 26–35], and Table S2). By contrast, Ag-ESCs behaved as expected for cells with two paternal genomes as 8 out of 12 PEGs were more expressed and 6 out of 7 MEGs were less expressed in Ag-ESCs compared to Bp-ESCs (Fig. 1A, B), confirming previous findings [27, 34, 47]. The seven BA genes were similarly expressed in Pg-ESCs and Bp-ESCs, as expected and only *Igf2r* was differentially expressed in Ag-ESCs compared to Bp-ESCs (Fig. 1C, S3). The expression levels of most imprinted genes varied between individual ESC lines of the same

genotype (Fig. S3), even within the two Bp-ESC lines. Culture conditions could account for this variability [56]. However, despite this noticeable variability, the Bp-like expression levels of all tested imprinted genes except *H19* (Fig. 1A, B) were still evident when considering the three Pg-ESC lines individually (Fig. S3). Thus, our results show that the expression levels of most imprinted genes in Pg-ESCs resembled those measured in Bp-ESCs whereas Ag-ESCs largely retained the altered expression levels of imprinted genes expected for cells with two paternal genomes.

DNA methylation distinguishes both parental alleles on differentially methylated regions (DMRs) at imprinted loci and affects the expression levels of imprinted genes [21]. We therefore quantified DNA methylation, using an assay based on qPCR and McrBC, a methylation-sensitive enzyme [57]. We validated this assay on two control DNA regions in all seven ESC lines (Fig. S4) and measured the methylation levels of nine imprinted DMRs [21] (Fig. S5A, B). As observed for transcription levels, DNA methylation levels varied between lines. Notably, methylation levels of the E14 Bp-ESC line were globally lower than the expected 50% (Fig. S5A, B), confirming our findings using RRBS [37]. However, despite the variability between lines, there were some noticeable trends. First, in the two Ag-ESC lines, methylation was absent at 2 out of 3 maternal DMRs and the 6 paternal DMRs were highly methylated (Fig S5A, B). In the three Pg-ESC lines, the two most affected DMRs were IG-DMR and H19-DMR (Fig. S5A, B). Bisulfite sequencing of clones confirmed that methylation of individual CpGs at these two paternal DMRs was lower in Pg-ESCs compared to Bp-ESCs (Fig. S5C, D), as previously reported [35, 58].

Collectively, these findings show that Pg-ESCs did not maintain the pattern of expression for imprinted genes expected for cells with two maternal genomes. Instead, Pg-ESC imprinting (expression levels of imprinted genes and methylation at DMRs) largely resembled Bp-ESC imprinting. By contrast, Ag-ESC imprinting was consistent with cells harboring two paternal genomes.

Pg-ESCs generate electrophysiologically active cortical-like neurons in vitro

We next investigated whether Pg-ESCs generated functional cortical-like derivatives. We differentiated the seven Pg-, Ag- and Bp-lines according to a validated protocol of in vitro corticogenesis [51]. We studied the expression of cortical and non-cortical markers at mid-corticogenesis (d12) and at the end of neurogenesis (d21) [2]. The two Pg-ESC lines Pg-BT6 and Pg-08-21 consistently gave derivatives (n=4/4 experiments) while the third Pg-ESC line (PR8) gave derivatives in 2/4 attempts (cells died in the two failed attempts, not shown). At d12, all lines generated rosettes containing NESTIN⁺PAX6⁺ cells, a feature of cortical progenitors (Fig. 2A–F). To get qualitative insights into the identity of the derivatives of Pg-ESCs and Ag-ESCs, we next performed RT-qPCR for a large repertoire of markers of cortical and non-cortical fates. Expression levels were normalized to that of E14, the gold standard for corticogenesis from mouse ESCs [2]. Of note, the expression levels of markers varied between lines of the same genotype, including between the two Bp lines as reflected by large error bars (Fig. 2G, H and S6). At d12, the expression levels of 15/16 cortical markers, including *Pax6*, *Tbr1*, *Reln*, and *Bcl11b*, were similar in Pg-ESCs and Bp-ESCs derivatives (Fig. 2G, Fig. S6A and not shown) and only *Pou3f2* was differentially expressed

(Fig. S6A). The expression levels of proliferation markers were also similar (Fig. S6B) and markers of non-cortical fates were not different or lower in Pg than in Bp-ESC derivatives (Fig. S6C). After 21 days of corticogenesis, all 16 cortical and neural markers were similarly expressed between Pg and Bp derivatives (Fig. 2H, Fig. S6D). By contrast, the expression levels of five genes essential for corticogenesis at d12 (Fig. 2G, Fig. S6A) and of *Foxg1* at d21 (Fig. 2H, Fig. S6D, and not shown) were lower in Ag-ESC than in Bp-ESC derivatives. Immunostaining confirmed the expression of specific markers of cortical layers [59] in Ag- and Pg-ESC derivatives: REELIN, TBR1, BCL11B and POU3F2 (Fig. 2I–T). Thus, qualitatively, Pg-ESCs and Ag-ESCs generated cells that express markers of *bona fide* cortical progenitors and neurons.

We next determined whether uniparental ESC-derived neurons were glutamatergic and biologically active, as reported for Bp-ESC-derived cortical neurons [2]. After four weeks in culture, Pg and Ag neurons expressed the synaptic marker HOMER1 (Fig. S7A–C). To get insight into the synaptic maturity and glutamatergic identity of uniparental neurons, we performed patch-clamp recordings. As Bp neurons, Ag and Pg neurons fired action potentials with a slow rising phase (Fig. 2U). Glutamatergic receptor antagonists (CNQX and AP5, Fig. 2V) blocked the miniature excitatory post-synaptic currents evoked by Bp, Ag and Pg neurons while we did not record any inhibitory GABAergic miniature event (not shown). This indicates that Bp, Pg and Ag neurons used glutamate as a neurotransmitter. Three other electrophysiological properties (Fig. S7D–F), including resting membrane potential (Fig. S7D), were also comparable between Bp and uniparental neurons. Thus, Pg-ESCs and Ag-ESCs produced mature, glutamatergic, cortical-like neurons.

Pg cortical-like cells maintain the biparental-like expression levels of most imprinted genes

We next assessed whether differentiated Pg cells maintained the Bp-like imprinting of undifferentiated Pg-ESCs. We quantified in Pg, Ag and Bp derivatives the expression levels of 34 genes identified as PEGs (19 genes), MEGs (10 genes) or BA (5 genes) at d12 and d21 of corticogenesis [37]. At d12, three PEGs and two MEGs (out of 29) were differentially expressed (adjusted- $p < 0.05$) between Pg and Bp derivatives (Fig. 3A, B). At d21, only *Dlk1*, which shifts from a biallelic expression in ESCs to a paternal expression in differentiated cells [37, 57], was differentially expressed (Fig. 3D, E). *H19* and *Igf2* were close to be significantly differentially expressed (adjusted- $p = 0.06$). In contrast to Pg derivatives, 11 PEGs and 7 MEGs at d12 (Fig. 3A, B) and 8 PEGs and 8 MEGs at d21 (Fig. 3D, E) were differentially expressed in Ag compared to Bp derivatives with expected higher expressing PEGs and lower expressing MEGs. There was no difference in the expression levels of the 5 BA genes between Bp and Pg or Ag derivatives (Fig. 3C, F). Although the expression levels of some imprinted genes varied between lines, the global trend of Bp-like expression of imprinted genes did occur in the two individual Pg-ESC lines for which we had at least three differentiated samples (Fig. S8). We conclude that cortical-like Pg derivatives maintained the Bp-like expression of most imprinted genes whereas Ag derivatives maintained their Ag-like expression pattern.

Pg-ESC derivatives contribute to the cortical lineage during in vivo development

We next investigated whether Pg-ESC derivatives contribute to the cortical lineage in vivo. We produced chimeras by injecting GFP⁺ Pg-, Ag- or Bp-ESCs into C57BL/6 blastocysts, followed by embryo transfer into pseudo pregnant CD-1 mice. We analyzed the presumptive cortex (dorsal telencephalon) of 8 Pg, 7 Ag and 4 Bp chimeras at E12.5. The gross morphology of heads of all Pg chimeras was normal whereas two heads of Ag chimeras were overgrown (Table S3). The contribution of ESC derivatives (i.e. the amount of GFP⁺ cells) varied between animals and independently of their genotype (not shown). This likely reflects the known stochastic contribution of ESCs in chimeras [60]. Importantly, the cortex of all Pg and all Bp chimeras contained GFP⁺ cells, (Fig. 4A–C, G–I, Table S3), indicative of substantial contribution of Pg derivatives to the mouse cortex, as reported [38]. Six out of seven Ag chimeras had GFP⁺ cells in the cortex (Fig. 4D–F, Table S3). There was no apparent difference in the distributions of uniparental and Bp derivatives in the cortex (Table S3) and most cells had the expected radial orientation [61] (Fig. 4J–L). We next determined whether the derivatives of uniparental ESCs expressed cortical markers at the expected locations. Uniparental derivatives expressed the cortical progenitor marker NGN2 (Fig. 5A–I, Fig. S9 and Table S3), at the expected intermediate zone [62]. All Pg chimeras but only 4/6 Ag chimeras had some GFP⁺NGN2⁺ cells (Table S3). The spatial distribution of NGN2⁺ cells looked similar and restricted to the dorsal telencephalon (Fig. S9), suggesting that the dorsal and ventral territories were properly established in the telencephalon of Pg and Ag chimeras. In addition to NGN2⁺ cortical progenitors, the E12.5 cortex contains TBR1⁺ pioneer neurons and BCL11B⁺ deep layer neurons [59]. These neurons are in a thin cortical plate, under the marginal zone, which contains REELIN⁺ cells [59]. We retrieved Pg and Ag GFP⁺ with the typical punctate REELIN staining at the expected marginal zone and TBR1⁺ and BCL11B⁺ cells that seemed properly located in the cortical plate (Fig. 5J–R). There were Pg cells positive for each cortical marker in all examined brain sections (Table S3) but not for all Ag chimeras (Table S3). We conclude that Pg-ESC derivatives participated efficiently to the cortical lineage at E12.5 and that Ag-ESC contributed less.

Transplanted Pg-ESC derivatives integrate into the injured adult cerebral cortex

We next followed the behavior of grafted Pg-ESC derivatives in an established model of cortical injury [63]. Lesions were made in the right rostral part of the cortex (primary motor and somatosensory areas) and in the left caudal (visual) cortex of adult mice (n=21). Pg- and control Bp-ESC lines were differentiated for 13–16 days in vitro and their cortical-like derivatives were injected into the freshly lesioned cortex. Two-week post-grafting, we searched for the presence of grafts by imaging the whole brains under a fluorescent stereomicroscope (Fig. 6A–I). Most mice had a GFP⁺ transplant in their visual cortex (7/8 animals for Pg and 5/13 for Bp, Table S4). The visual cortex was more efficiently targeted than the motor cortex (Fig. 6A–C and Table S4), as previously reported for Bp-ESCs [3]. Most transplants were correctly located, close to the lesion (Fig. 6A–I and Table S4). Only one animal had a visible teratoma (not shown), a proportion consistent with previous findings using Bp-ESCs [3]. To better characterize the transplants, we performed GFP immunostaining on free-floating sections. We confirmed the presence of GFP⁺ grafts and discovered additional small grafts in animals previously found negative when analyzed by stereomicroscope (Table S4). The size of Bp and Pg transplants was variable, ranging from a

partial reconstitution for most animals (Fig. 6J–O and Table S4) to a large reconstitution of the lesion cavity in a few cases (Fig. S10).

To get insight into the molecular identity of transplants and to trace their axonal projections, we performed immunostainings. Transplants contained numerous neurons (TUBB3⁺, Fig. 6P, S), surrounded by host astrocytes (Fig. 6Q, T), as reported for Bp-ESC cortical transplants [3]. Some GFP⁺ cells within Pg and Bp transplants expressed the cortical marker POU3F2 (Fig. 6R, U). There were no TBR1⁺ cells (not shown). Importantly, both Bp and Pg transplanted neurons sent numerous GFP⁺ axons (Fig. 7A, B and Table S4). Some axons ended by a growth cone (Fig. 7I, J), which suggests they were developing immature axons looking for their target regions. Pg axonal projections seemed to follow specific cortical paths as previously reported for animals after two weeks of transplantation with Bp-ESC cortical-like derivatives [3]. Pg and Bp GFP⁺ axons notably invaded the corpus callosum (Fig. 7C, D). Some axons crossed the midline (Fig. 7C, D) to reach the contralateral cortex (Fig. 7E, F) at several hundred microns away from the transplanted neurons. In addition to these cortico-cortical projections, in a few cases Pg and Bp transplants also sent subcortical projections, as evidenced by the presence of GFP⁺ projections into the striatum (Fig. 7G, H, and Table S4).

Thus, the cortical-like derivatives of Pg-ESC integrated into the injured adult cortex and they sent axons with a pattern of projection typical of cortical neurons.

Discussion

Here, we show that the expression levels of most imprinted genes in three mouse Pg-ESC lines resemble those of Bp-ESCs. Importantly, Pg-ESC cortical-like derivatives maintain this biparental-like expression. In addition, Pg-ESCs generate cortical-like neurons that are functional. Finally, Pg-ESC derivatives integrate properly in the developing cortex and in the injured adult cerebral cortex. Collectively, this supports the utility of Pg-ESCs derivatives for neocortical repair.

Previous studies have shown that Pg-ESCs display enhanced expression of some MEGs and reduced expression of some PEGs. However, biparental expression of at least a subset of imprinted genes is frequently observed ([18, 26–35], and Table S2). The expression levels of imprinted genes greatly vary between Pg-ESC lines [32, 64]. Similarly, we detected variability between ESC lines. Despite this variability, we found that Pg-ESC lines had a Bp-like expression of most imprinted genes, in sharp contrast with Ag-ESC lines. Notably the expression of many MEGs is lost in Ag cells whereas the expression of a few PEGs is reduced but not lost in Pg-ESCs. The reason for biparental-like expression of imprinted genes in Pg-ESCs is largely unknown. Li et al. [35] showed that the process of in vitro culture alters the expression levels of many PEGs and methylation levels at some DMRs. In contrast to this global biparental-like behavior, we observed that two imprinted loci behaved as expected: the two paternal DMRs Ig-DMR and H19-DMR were hypomethylated as previously reported [35], with two high expressing MEGs (*Mirg* and *H19*, but not *Meg3*) and two low expressing PEGs (*Dlk1* and *Igf2*) at d21. Interestingly, the genetic manipulation of these two imprinted loci is sufficient to generate parthenogenetic mice [65]. To our

knowledge, the long-term consequences of a deregulation of these two imprinted loci are unknown but given the roles of imprinted genes transcribed from these loci on proliferation [53] and stem cells [23, 66], teratoma formation should be checked when performing grafting experiments with Pg-ESC derivatives. Alternatively, the expression levels of genes located in the H19-Igf2 and Dlk1-Dio3 loci might be manipulated in Pg-ESCs so that they approach those of Bp-ESCs. For instance, a shRNA against H19 reduces its expression level while promoting cardiomyogenesis in Pg-ESCs [31]. Embryo aggregation also greatly improves the fidelity of imprinted gene expression of Pg-ESCs [67].

Despite these high expressing *H19* and low expressing *Igf2* and *Dlk1*, our Pg-ESCs lines generated cells with typical cortical features. Pg-ESCs were differentiated according to a corticogenesis protocol that is based on a minimalistic ‘by default’ media [51], which suggests that by default Pg-ESCs differentiate into cortical-like derivatives, as reported for Bp-ESCs [2]. However, because the expression levels of cortical markers varied, even between the two Bp-ESC lines, we cannot conclude on the efficiency of this process. Two out of three Pg-ESC lines reproducibly generated cortical-like derivatives, suggesting that most mouse Pg-ESC lines have the capacity to generate cortical-like derivatives. Our in vitro studies also show that Pg-ESCs generated cortical-like neurons that were glutamatergic and electrophysiologically active. In vivo, Pg-ESCs participated to the cortical lineage in fetal chimeras. Finally, transplanted Pg-ESC derivatives integrated well into the injured adult cortex with Pg transplants sending long-range projections typical of cortical neurons. It will be important in the future to determine how these projections mature within the host brain and if they can improve the state of injured cerebral cortex.

In contrast to Pg-ESCs, Ag-ESCs largely retained the expression levels of imprinted genes expected for cells with two paternal genomes, which may be a roadblock for their future use in cell grafting experiments. Screening of several Ag-ESC lines may result in a line having Bp-like imprinting but our data and those of others [27, 34, 47] suggest that such a line might be difficult to find. Despite their imprinting status, we found that Ag-ESCs generated cortical-like cells in vitro and in embryonic chimeras, confirming and extending previous findings [47]. This suggests that either imprinting is not crucial for corticogenesis or that Ag-ESCs adopt compensatory mechanisms. However, the cortical potential of Ag might be lower than that of Bp and Pg-ESCs as five cortical markers were less expressed in Ag than in Bp derivatives in vitro. Additionally, 2/7 Ag chimeras had no or little contribution to cortex, while there was a good contribution for all Pg chimeras (8/8 animals). Thus, the cortical potential of Ag- might be lower than that of Pg-ESC derivatives, as suggested earlier by Keverne and coworkers [68].

Finally, the ultimate objective of using Pg-ESC derivatives for cortical therapy requires investigating whether human Pg-ESCs have the same biparental-like imprinting and potency to differentiate into cortical-like neurons. Few data are available on the imprinting status of human Pg-ESC lines but it was reported that their imprinting is not Bp-like [15, 69]. Considering variability between human ESC lines [70], screening numerous human Pg-ESC lines could possibly identify Pg lines with Bp-like imprinting. Human Pg-ESCs can be specified into functional neurons [15], including dopaminergic neurons [71], which indicates that they could be certainly oriented toward the cortical lineage. Ultimately, these human

cortical-like Pg neurons should be grafted into mouse cortex to determine how they integrate into the host circuitry, as previously reported for neurons derived from human Bp-ESCs [4], and whether they restore cortical functions.

Summary

Pg-ESCs generate functional cortical neurons with a biparental-like imprinting and Pg-ESC derivatives integrate properly in the embryonic cortex and in the injured adult cortex. Our study therefore increases the utility of Pg-ESC derivatives for cellular therapies, including neocortex repair.

Supplementary Material

Refer to Web version on PubMed Central for supplementary material.

Acknowledgments

We thank Afsaneh Gaillard for advice on grafting experiments and helpful comments on our manuscript. We thank Pierre Vanderhaeghen for advice on grafting experiments. We thank Robert Feil for the uniparental AK2 and PR8 ESC lines and Yves-Alain Barde for the Tau-GFP ESC line. We thank Chrystel Lafont (small animal imaging platform of Montpellier, IPAM, <http://www.ipam.cnrs.fr/>) for taking pictures at the stereomicroscope. We thank William Ritchie for help with statistical analysis and comments on our manuscript. We thank Francis Rubio for technical assistance with animals and Coleen Roger for vibrosections. We thank Hala Al Adhami, Pierre-François Méry and colleagues of the Oncology department for helpful discussions.

This work was funded by an ANR grant Epinet (to L.J.) and NIH Grants 1RO3 HD045291-01 and 1RO1 DK080852 (to K.J.M.). B.G. was supported by a grant from the French Ministère de la Recherche et des Technologies.

References

1. Bazarek S, Peterson DA. Prospects for engineering neurons from local neocortical cell populations as cell-mediated therapy for neurological disorders. *The Journal of comparative neurology*. 2014; 522:2857–2876. [PubMed: 24756774]
2. Gaspard N, Bouschet T, Hourez R, et al. An intrinsic mechanism of corticogenesis from embryonic stem cells. *Nature*. 2008; 455:351–357. [PubMed: 18716623]
3. Michelsen KA, Acosta-Verdugo S, Benoit-Marand M, et al. Area-specific reestablishment of damaged circuits in the adult cerebral cortex by cortical neurons derived from mouse embryonic stem cells. *Neuron*. 2015; 85:982–997. [PubMed: 25741724]
4. Espuny-Camacho I, Michelsen KA, Gall D, et al. Pyramidal neurons derived from human pluripotent stem cells integrate efficiently into mouse brain circuits in vivo. *Neuron*. 2013; 77:440–456. [PubMed: 23395372]
5. Barker RA, Widner H. Immune problems in central nervous system cell therapy. *NeuroRx*. 2004; 1:472–481. [PubMed: 15717048]
6. Weinger JG, Weist BM, Plaisted WC, et al. MHC mismatch results in neural progenitor cell rejection following spinal cord transplantation in a model of viral-induced demyelination. *Stem Cells*. 2012; 30:2584–2595. [PubMed: 22969049]
7. Taylor CJ, Bolton EM, Bradley JA. Immunological considerations for embryonic and induced pluripotent stem cell banking. *Philos Trans R Soc Lond B Biol Sci*. 2011; 366:2312–2322. [PubMed: 21727137]
8. Ohnuki M, Takahashi K. Present and future challenges of induced pluripotent stem cells. *Philos Trans R Soc Lond B Biol Sci*. 2015; 370:20140367. [PubMed: 26416678]
9. Surani MA, Barton SC, Norris ML. Development of reconstituted mouse eggs suggests imprinting of the genome during gametogenesis. *Nature*. 1984; 308:548–550. [PubMed: 6709062]

10. Kim K, Lerou P, Yabuuchi A, et al. Histocompatible embryonic stem cells by parthenogenesis. *Science*. 2007; 315:482–486. [PubMed: 17170255]
11. Revazova ES, Turovets NA, Kochetkova OD, et al. HLA homozygous stem cell lines derived from human parthenogenetic blastocysts. *Cloning Stem Cells*. 2008; 10:11–24. [PubMed: 18092905]
12. Nakajima F, Tokunaga K, Nakatsuji N. Human leukocyte antigen matching estimations in a hypothetical bank of human embryonic stem cell lines in the Japanese population for use in cell transplantation therapy. *Stem Cells*. 2007; 25:983–985. [PubMed: 17185611]
13. Schmitt J, Eckardt S, Schlegel PG, et al. Human Parthenogenetic Embryonic Stem Cell-Derived Neural Stem Cells Express HLA-G and Show Unique Resistance to NK Cell-Mediated Killing. *Mol Med*. 2015; 21:185–196. [PubMed: 25811991]
14. Turovets N, Semechkin A, Kuzmichev L, et al. Derivation of human parthenogenetic stem cell lines. *Methods Mol Biol*. 2011; 767:37–54. [PubMed: 21822866]
15. Ahmad R, Wolber W, Eckardt S, et al. Functional neuronal cells generated by human parthenogenetic stem cells. *PloS one*. 2012; 7:e42800. [PubMed: 22880113]
16. Sanchez-Pernaute R, Studer L, Ferrari D, et al. Long-term survival of dopamine neurons derived from parthenogenetic primate embryonic stem cells (cyno-1) after transplantation. *Stem Cells*. 2005; 23:914–922. [PubMed: 15941857]
17. Espejel S, Eckardt S, Harbell J, et al. Brief report: Parthenogenetic embryonic stem cells are an effective cell source for therapeutic liver repopulation. *Stem Cells*. 2014; 32:1983–1988. [PubMed: 24740448]
18. Didie M, Christalla P, Rubart M, et al. Parthenogenetic stem cells for tissue-engineered heart repair. *The Journal of clinical investigation*. 2013; 123:1285–1298. [PubMed: 23434590]
19. Eckardt S, Leu NA, Bradley HL, et al. Hematopoietic reconstitution with androgenetic and gynogenetic stem cells. *Genes Dev*. 2007; 21:409–419. [PubMed: 17322401]
20. Liu W, Yin L, Yan X, et al. Directing the Differentiation of Parthenogenetic Stem Cells Into Tenocytes for Tissue-Engineered Tendon Regeneration. *Stem cells translational medicine*. 2016
21. Ferguson-Smith AC. Genomic imprinting: the emergence of an epigenetic paradigm. *Nat Rev Genet*. 2011; 12:565–575. [PubMed: 21765458]
22. Wilkinson LS, Davies W, Isles AR. Genomic imprinting effects on brain development and function. *Nature reviews Neuroscience*. 2007; 8:832–843. [PubMed: 17925812]
23. Plasschaert RN, Bartolomei MS. Genomic imprinting in development, growth, behavior and stem cells. *Development*. 2014; 141:1805–1813. [PubMed: 24757003]
24. Holm TM, Jackson-Grusby L, Brambrink T, et al. Global loss of imprinting leads to widespread tumorigenesis in adult mice. *Cancer Cell*. 2005; 8:275–285. [PubMed: 16226703]
25. Kim J, Bretz CL, Lee S. Epigenetic instability of imprinted genes in human cancers. *Nucleic Acids Res*. 2015
26. Allen ND, Barton SC, Hilton K, et al. A functional analysis of imprinting in parthenogenetic embryonic stem cells. *Development*. 1994; 120:1473–1482. [PubMed: 8050357]
27. Cui XS, Shen XH, Sun SC, et al. Identifying MicroRNA and mRNA expression profiles in embryonic stem cells derived from parthenogenetic, androgenetic and fertilized blastocysts. *J Genet Genomics*. 2013; 40:189–200. [PubMed: 23618402]
28. Hikichi T, Kohda T, Wakayama S, et al. Nuclear transfer alters the DNA methylation status of specific genes in fertilized and parthenogenetically activated mouse embryonic stem cells. *Stem Cells*. 2008; 26:783–788. [PubMed: 18192228]
29. Jang HS, Hong YJ, Choi HW, et al. Changes in Parthenogenetic Imprinting Patterns during Reprogramming by Cell Fusion. *PloS one*. 2016; 11:e0156491. [PubMed: 27232503]
30. McKarney LA, Overall ML, Dziadek M. Myogenesis in cultures of uniparental mouse embryonic stem cells: differing patterns of expression of myogenic regulatory factors. *The International journal of developmental biology*. 1997; 41:485–490. [PubMed: 9240565]
31. Ragina NP, Schlosser K, Knott JG, et al. Downregulation of H19 improves the differentiation potential of mouse parthenogenetic embryonic stem cells. *Stem Cells Dev*. 2012; 21:1134–1144. [PubMed: 21793658]

32. Sturm KS, Berger CN, Zhou SX, et al. Unrestricted lineage differentiation of parthenogenetic ES cells. *Dev Genes Evol.* 1997; 206:377–388. [PubMed: 27747399]
33. Shan ZY, Wu YS, Shen XH, et al. Aggregation of pre-implantation embryos improves establishment of parthenogenetic stem cells and expression of imprinted genes. *Dev Growth Differ.* 2012; 54:481–488. [PubMed: 22435468]
34. Szabo P, Mann JR. Expression and methylation of imprinted genes during in vitro differentiation of mouse parthenogenetic and androgenetic embryonic stem cell lines. *Development.* 1994; 120:1651–1660. [PubMed: 8050371]
35. Li C, Chen Z, Liu Z, et al. Correlation of expression and methylation of imprinted genes with pluripotency of parthenogenetic embryonic stem cells. *Hum Mol Genet.* 2009; 18:2177–2187. [PubMed: 19324901]
36. Prickett AR, Oakey RJ. A survey of tissue-specific genomic imprinting in mammals. *Mol Genet Genomics.* 2012; 287:621–630. [PubMed: 22821278]
37. Bouschet T, Dubois E, Reynes C, et al. In Vitro Corticogenesis from Embryonic Stem Cells Recapitulates the In Vivo Epigenetic Control of Imprinted Gene Expression. *Cereb Cortex.* 2017; 27:2418–2433. [PubMed: 27095822]
38. Allen ND, Logan K, Lally G, et al. Distribution of parthenogenetic cells in the mouse brain and their influence on brain development and behavior. *Proceedings of the National Academy of Sciences of the United States of America.* 1995; 92:10782–10786. [PubMed: 7479883]
39. Mairet-Coello G, Tury A, Van Buskirk E, et al. p57(KIP2) regulates radial glia and intermediate precursor cell cycle dynamics and lower layer neurogenesis in developing cerebral cortex. *Development.* 2012; 139:475–487. [PubMed: 22223678]
40. Adnani L, Langevin LM, Gautier E, et al. Zac1 Regulates the Differentiation and Migration of Neocortical Neurons via Pac1. *The Journal of neuroscience : the official journal of the Society for Neuroscience.* 2015; 35:13430–13447. [PubMed: 26424889]
41. Ferron SR, Charalambous M, Radford E, et al. Postnatal loss of Dlk1 imprinting in stem cells and niche astrocytes regulates neurogenesis. *Nature.* 2011; 475:381–385. [PubMed: 21776083]
42. Lehtinen MK, Zappaterra MW, Chen X, et al. The cerebrospinal fluid provides a proliferative niche for neural progenitor cells. *Neuron.* 2011; 69:893–905. [PubMed: 21382550]
43. Chamberlain SJ, Lalonde M. Angelman syndrome, a genomic imprinting disorder of the brain. *The Journal of neuroscience : the official journal of the Society for Neuroscience.* 2010; 30:9958–9963. [PubMed: 20668179]
44. Mackay DJ, Callaway JL, Marks SM, et al. Hypomethylation of multiple imprinted loci in individuals with transient neonatal diabetes is associated with mutations in ZFP57. *Nature genetics.* 2008; 40:949–951. [PubMed: 18622393]
45. Eggermann T, Perez de Nanclares G, Maher ER, et al. Imprinting disorders: a group of congenital disorders with overlapping patterns of molecular changes affecting imprinted loci. *Clinical epigenetics.* 2015; 7:123. [PubMed: 26583054]
46. Mann JR, Gadi I, Harbison ML, et al. Androgenetic mouse embryonic stem cells are pluripotent and cause skeletal defects in chimeras: implications for genetic imprinting. *Cell.* 1990; 62:251–260. [PubMed: 2372828]
47. Dinger TC, Eckardt S, Choi SW, et al. Androgenetic embryonic stem cells form neural progenitor cells in vivo and in vitro. *Stem Cells.* 2008; 26:1474–1483. [PubMed: 18369101]
48. Tucker KL, Meyer M, Barde YA. Neurotrophins are required for nerve growth during development. *Nat Neurosci.* 2001; 4:29–37. [PubMed: 11135642]
49. Khosla S, Aitchison A, Gregory R, et al. Parental allele-specific chromatin configuration in a boundary-imprinting-control element upstream of the mouse H19 gene. *Mol Cell Biol.* 1999; 19:2556–2566. [PubMed: 10082521]
50. Eckardt S, Leu NA, Yanchik A, et al. Gene therapy by allele selection in a mouse model of beta-thalassemia. *The Journal of clinical investigation.* 2011; 121:623–627. [PubMed: 21293060]
51. Gaspard N, Bouschet T, Herpoel A, et al. Generation of cortical neurons from mouse embryonic stem cells. *Nature protocols.* 2009; 4:1454–1463. [PubMed: 19798080]
52. Nagy, A. *Manipulating the mouse embryo: A Laboratory Manual.* 3. Cold Spring Harbor Laboratory Press; 2003.

53. Al Adhami H, Evano B, Le Digarcher A, et al. A systems-level approach to parental genomic imprinting: the imprinted gene network includes extracellular matrix genes and regulates cell cycle exit and differentiation. *Genome Res.* 2015; 25:353–367. [PubMed: 25614607]
54. Chambers I, Silva J, Colby D, et al. Nanog safeguards pluripotency and mediates germline development. *Nature.* 2007; 450:1230–1234. [PubMed: 18097409]
55. Hernandez L, Kozlov S, Piras G, et al. Paternal and maternal genomes confer opposite effects on proliferation, cell-cycle length, senescence, and tumor formation. *Proceedings of the National Academy of Sciences of the United States of America.* 2003; 100:13344–13349. [PubMed: 14581617]
56. Greenberg MV, Bourc'his D. Cultural relativism: maintenance of genomic imprints in pluripotent stem cell culture systems. *Curr Opin Genet Dev.* 2015; 31:42–49. [PubMed: 25974256]
57. Kota SK, Lleres D, Bouschet T, et al. ICR noncoding RNA expression controls imprinting and DNA replication at the Dlk1-Dio3 domain. *Developmental cell.* 2014; 31:19–33. [PubMed: 25263792]
58. Hikichi T, Wakayama S, Mizutani E, et al. Differentiation potential of parthenogenetic embryonic stem cells is improved by nuclear transfer. *Stem Cells.* 2007; 25:46–53. [PubMed: 17008422]
59. Molyneaux BJ, Arlotta P, Menezes JR, et al. Neuronal subtype specification in the cerebral cortex. *Nature reviews Neuroscience.* 2007; 8:427–437. [PubMed: 17514196]
60. Eckardt S, McLaughlin KJ, Willenbring H. Mouse chimeras as a system to investigate development, cell and tissue function, disease mechanisms and organ regeneration. *Cell cycle.* 2011; 10:2091–2099. [PubMed: 21606677]
61. Sun T, Hevner RF. Growth and folding of the mammalian cerebral cortex: from molecules to malformations. *Nature reviews Neuroscience.* 2014; 15:217–232. [PubMed: 24646670]
62. Fode C, Ma Q, Casarosa S, et al. A role for neural determination genes in specifying the dorsoventral identity of telencephalic neurons. *Genes Dev.* 2000; 14:67–80. [PubMed: 10640277]
63. Gaillard A, Prestoz L, Dumartin B, et al. Reestablishment of damaged adult motor pathways by grafted embryonic cortical neurons. *Nat Neurosci.* 2007; 10:1294–1299. [PubMed: 17828256]
64. Gong SP, Kim H, Lee EJ, et al. Change in gene expression of mouse embryonic stem cells derived from parthenogenetic activation. *Hum Reprod.* 2009; 24:805–814. [PubMed: 19106175]
65. Kawahara M, Wu Q, Takahashi N, et al. High-frequency generation of viable mice from engineered bi-maternal embryos. *Nature biotechnology.* 2007; 25:1045–1050.
66. Peng F, Li TT, Wang KL, et al. H19/let-7/LIN28 reciprocal negative regulatory circuit promotes breast cancer stem cell maintenance. *Cell Death Dis.* 2017; 8:e2569. [PubMed: 28102845]
67. Bai GY, Song SH, Wang ZD, et al. Embryos aggregation improves development and imprinting gene expression in mouse parthenogenesis. *Dev Growth Differ.* 2016; 58:270–279. [PubMed: 26991405]
68. Keverne EB, Fundele R, Narasimha M, et al. Genomic imprinting and the differential roles of parental genomes in brain development. *Brain Res Dev Brain Res.* 1996; 92:91–100. [PubMed: 8861727]
69. Lin G, OuYang Q, Zhou X, et al. A highly homozygous and parthenogenetic human embryonic stem cell line derived from a one-pronuclear oocyte following in vitro fertilization procedure. *Cell Res.* 2007; 17:999–1007. [PubMed: 18040289]
70. Rugg-Gunn PJ, Ferguson-Smith AC, Pedersen RA. Status of genomic imprinting in human embryonic stem cells as revealed by a large cohort of independently derived and maintained lines. *Hum Mol Genet.* 2007; 16(2):R243–251. [PubMed: 17911167]
71. Gonzalez R, Garitaonandia I, Crain A, et al. Proof of concept studies exploring the safety and functional activity of human parthenogenetic-derived neural stem cells for the treatment of Parkinson's disease. *Cell Transplant.* 2015; 24:681–690. [PubMed: 25839189]

The cerebral cortex is crucial for higher brain functions. There is no neurogenesis in the adult cortex to compensate for the loss of cortical neurons caused by disease or injury. Cortical-like neurons produced from normal, biparental (Bp) pluripotent cells, including mouse and human embryonic stem cells (ESCs), are a promising source of cortical transplants but their histocompatibility is limited. Parthenogenetic Pg-ESCs are more histocompatible ESCs but their application to cortical regeneration is unknown and their parental imprinting might be incompatible with therapy. We found that, in vitro, mouse Pg-ESCs generated progenitors and functional cortical-like neurons that displayed biparental-like expression of imprinted genes. In vivo, Pg-ESC derivatives integrated properly into the injured adult cortex. Our study therefore increases support for the utility of Pg-ESC derivatives for cellular therapies, including neocortex repair.

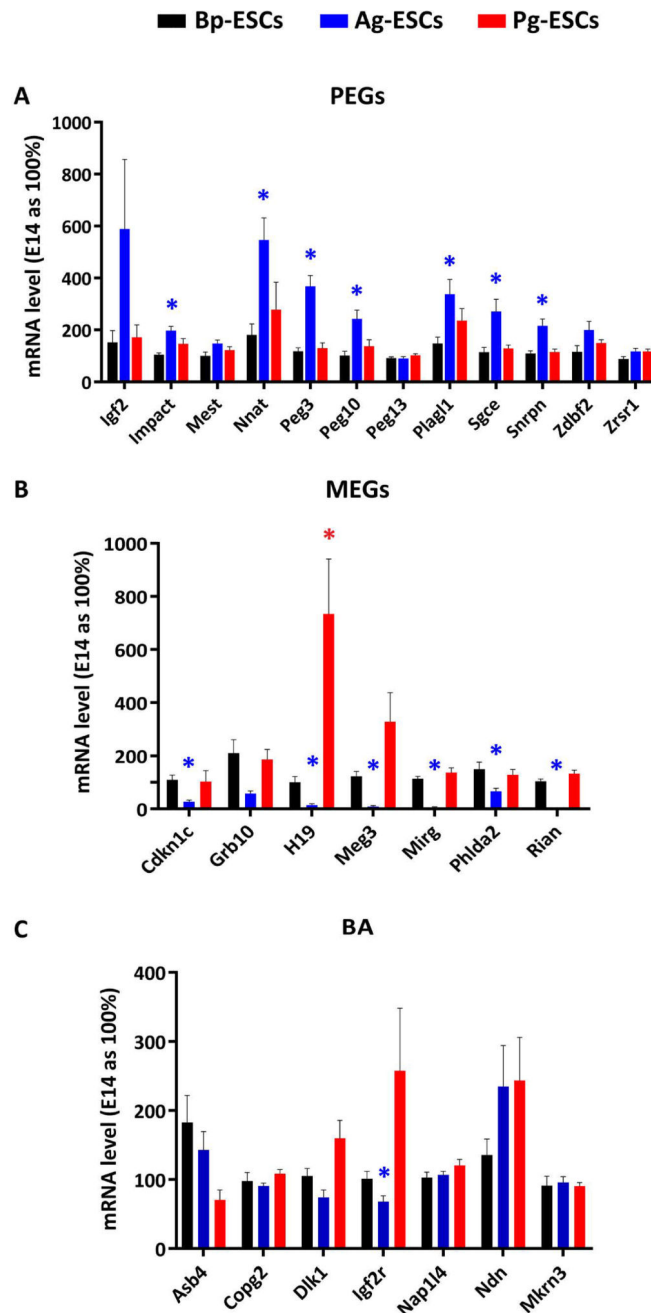


Fig. 1. Pg-ESCs display a biparental-like expression of imprinted genes

Quantification of the expression levels of 12 PEGs (**A**), 7 MEGs (**B**) and 7 biallelically expressed (BA) genes (**C**) in Bp-, Ag- and Pg-ESCs by RT-qPCR. RNAs were prepared from the 2 Bp lines (E14, n=7 and WT-B1, n=6), the 2 Ag lines (AK2, n=5 and AG-B6, n=6) and the 3 Pg lines (PR8, n=5, PG-BT6, n=4, and PG-08-021, n=4). Bar graphs show the mean + s.e.m. from the 13 Bp, 11 Ag and 13 Pg samples. Expression in the control E14 Bp-ESC line was taken as 100%. Expression levels in Pg vs. Bp and Ag vs. Bp ESCs were compared using a Mann-Whitney test followed by Benjamini-Hochberg correction for multiple tests. *, adjusted-p<0.05. Only *H19* was differentially expressed between Pg and

Bp lines while 6 MEGs and 7 PEGs were differentially expressed between Ag and Bp ESC lines.

Author Manuscript

Author Manuscript

Author Manuscript

Author Manuscript

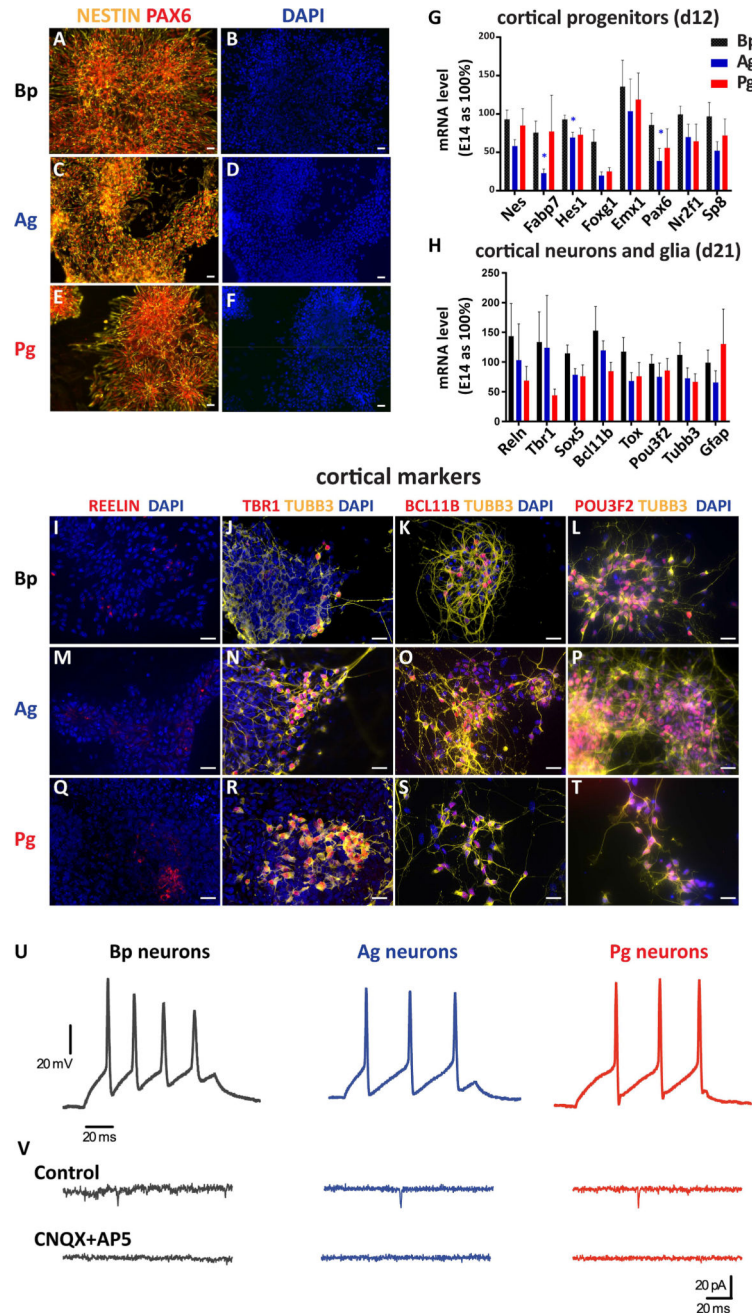


Fig. 2. Pg-ESCs generate electrophysiologically active cortical-like neurons in vitro
A–F. Immunostainings for the dorsal marker PAX6 (red), the neural progenitor marker NESTIN (yellow) and nuclei labeling (DAPI, blue) in the derivatives of Bp-ESCs, Ag-ESCs and Pg-ESCs at d12 of in vitro corticogenesis. Scale bars: 20 μ m. Data are representative of three independent experiments. Pictures shown are from E14, AG-B6 and Pg-BT6 lines. **G, H.** RT-qPCR quantification of the expression levels of markers of cortical progenitors (**G**) at d12 and of cortical neurons and layer markers at d21 (**H**) in Pg, Ag and Bp derivatives. Bar graphs show the mean + s.e.m. of Bp (E14, n=7 and WT-B1, n=5), Ag (AK2, n=5 and AG-B6, n=6) and Pg (PG-BT6, n=4, PR8, n=2 and PG-08-021, n=4) cells. Expression in the

control E14 Bp-ESC line was taken as 100%. A Mann-Whitney test followed by Benjamini-Hochberg correction for multiple tests was used. *: adjusted $p < 0.05$. **I–T**. Immunostaining for REELIN and TUBB3/TBR1 at d12 and TUBB3/BCL11B and TUBB3/POU3F2 at d21 of in vitro corticogenesis from E14 Bp-ESCs (**I–L**), Ag-BT6 (**M–P**) and PG-08-021 Pg-ESCs (**Q–T**). Nuclei are in blue (DAPI). Scale bars: 20 μm . Data are representative of three independent experiments. **U–V**. Electrophysiological analysis showing that Pg and Ag neurons are functional and glutamatergic. **U**. Example traces of action potentials recorded from 10 Bp, 15 Ag and 12 Pg-derived neurons from 3 independent cultures. **V**. Spontaneous excitatory post-synaptic currents evoked by Bp, Ag and Pg neurons were blocked by application of the glutamate receptor antagonists CNQX and AP5.

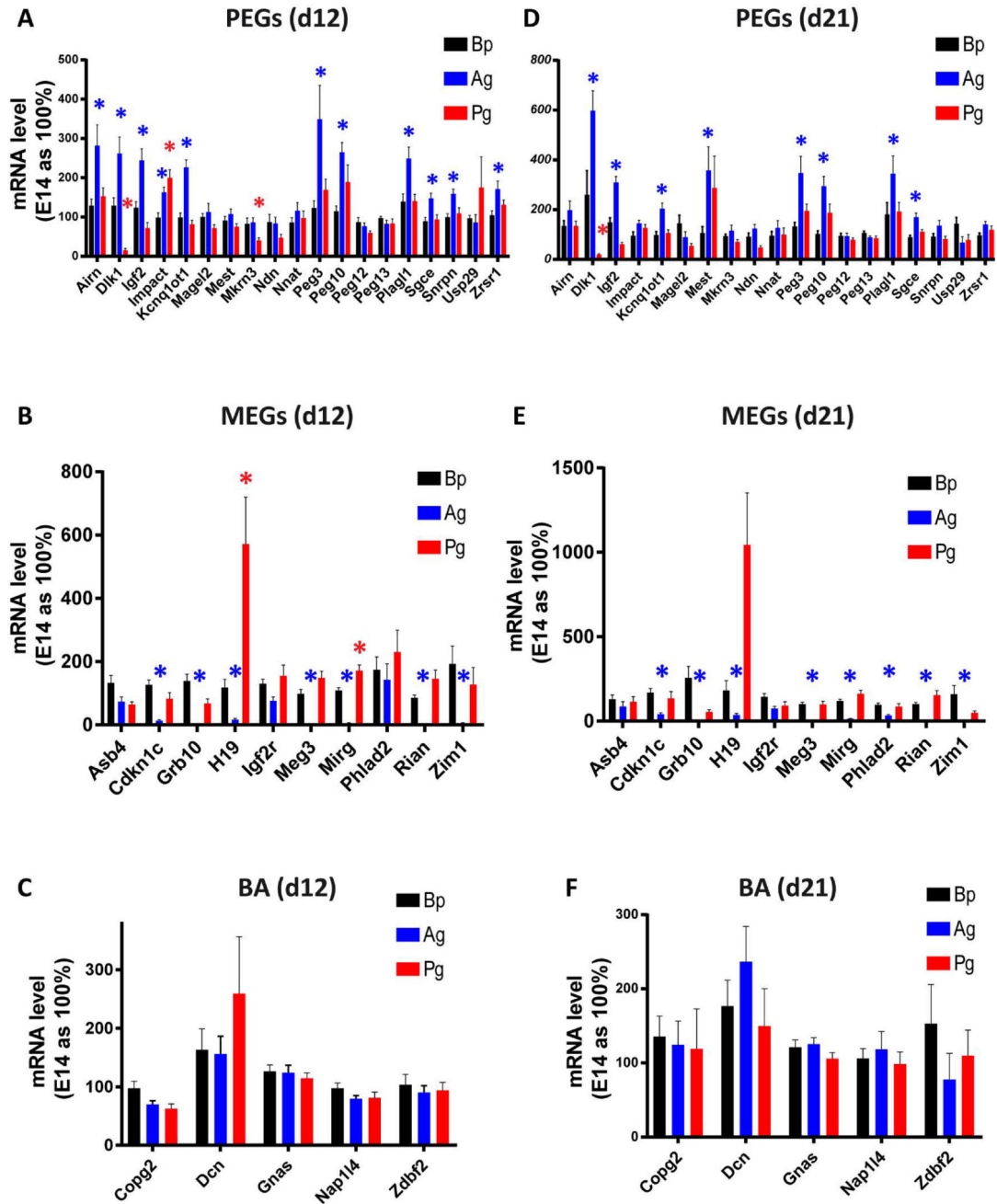


Fig. 3. Pg cortical-like cells maintain the biparental-like expression levels of most imprinted genes
 RT-qPCR quantification of the expression levels of 19 PEGs (**A, D**), 10 MEGs (**B, E**) and 5 BA genes (**C, F**) in Bp, Ag and Pg derivatives at d12 (**A–C**) and d21 (**D–F**) of in vitro corticogenesis. RNAs were prepared from the two Bp lines (E14, n=7 and WT-B1, n=6), the 2 Ag lines (AK2, n=5 and AG-B6, n=6) and the 3 Pg lines (PG-BT6, n=4, PR8, n=2 and PG-08-021, n=4) at d12 and d21. Bar graphs show the mean + s.e.m. from the 13 Bp, 11 Ag and 10 Pg samples. Data were normalized to the mean of E14 taken as 100%. *: adjusted-p<0.05. Note that at d21, only *Dlk1* was differentially expressed between Pg and Bp lines while 16 imprinted genes were differentially expressed between Ag and Bp derivatives.

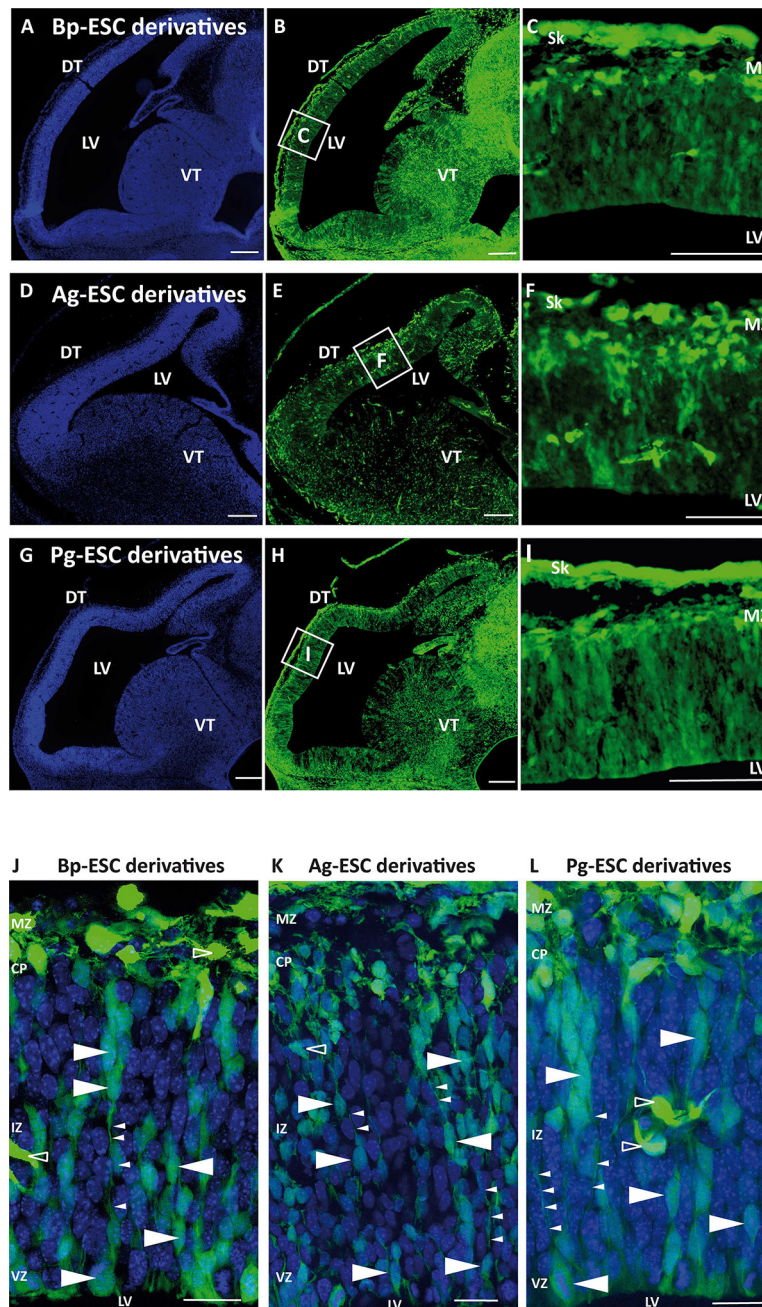


Fig. 4. Pg-ESC derivatives populate the developing cortex of chimeras and have a radial orientation

A–I. The GFP⁺ derivatives of Bp-ESCs (**A–C**), Ag-ESCs (**D–F**) and Pg-ESCs (**G–I**) localize to the dorsal and ventral telencephalons (DT and VT, respectively) of mouse chimeras at E12.5. Sections were stained with DAPI (blue). **C, F** and **I** panels are higher magnifications of selected areas in **B, E** and **H** panels respectively that show the presence of GFP⁺ cells in the DT of chimeras. LV: lateral ventricle, MZ: marginal zone, Sk: skin/skull. Scale bars: 200 μ m. **J–L.** Typical orientation of GFP⁺ derivatives of Bp-ESCs (**J**), Ag-ESCs (**K**) and Pg-ESCs (**L**) in the dorsal telencephalon of chimeras. Most uniparental-ESC derivatives had a

radial orientation (large arrowheads) and few had a tangential orientation (empty arrowheads). Some GFP⁺ cells sent processes typical of radial glia fibers (small arrowheads). The nuclear stain DAPI is in blue. LV: lateral ventricle, VZ: ventricular zone, IZ: intermediate zone, CP: cortical plate, MZ: marginal zone. Scale bars: 20 μ m. Data are representative of 4 Bp, 5 Ag and 8 Pg chimeras (see table S3).

Author Manuscript

Author Manuscript

Author Manuscript

Author Manuscript

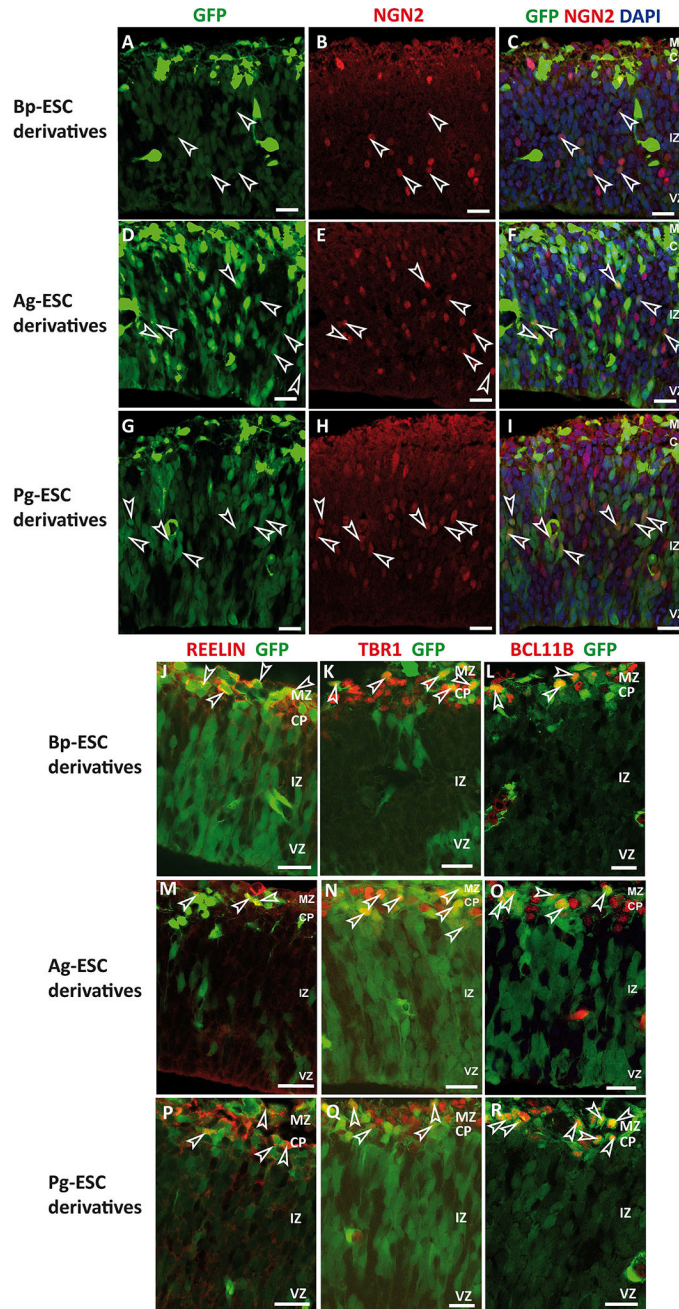


Fig. 5. Pg-ESC derivatives express markers of cortical progenitors and neurons in the fetal cortex

A–I. Triple labelling for ESC derivatives (GFP⁺, green), NGN2 (red), and the nuclear stain DAPI (blue) in the dorsal telencephalon of Bp (**A–C**), Ag (**D–F**) and Pg (**G–I**) chimeras at E12.5. Arrowheads indicate double-labelled GFP⁺ NGN2⁺ cells. Scale bars: 20 μm. NGN2⁺ GFP⁺ cells were observed in 4/4 Bp, 4/6 Ag and 7/7 Pg chimeras (see table S3). GFP⁺ cells in the dorsal telencephalon of Bp (**J–L**), Ag (**M–O**) and Pg (**P–R**) chimeras expressed REELIN (red) (**J, M, P**), the marker of pioneer cortical neurons TBR1 (red) (**K, N, Q**) and the deep layer marker BCL11B (red) (**L, O, R**). Arrowheads indicate GFP⁺ cells expressing

a given cortical marker. Scale bars: 20 μm . LV: lateral ventricle, VZ: ventricular zone, IZ: intermediate zone, CP: cortical plate, MZ: marginal zone.

Author Manuscript

Author Manuscript

Author Manuscript

Author Manuscript

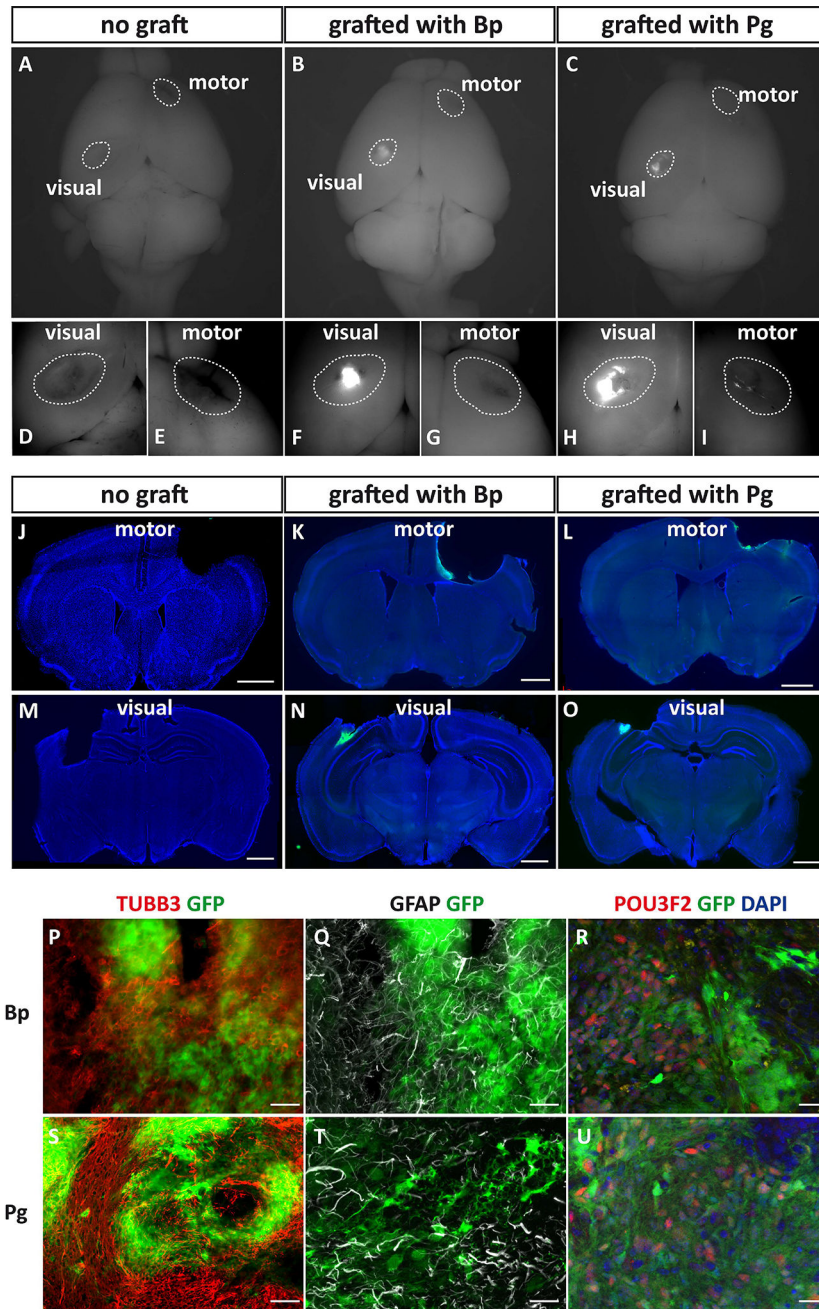


Fig. 6. Transplanted Pg-ESC derivatives integrate into the injured adult cerebral cortex
A–I. Illustrative pictures obtained at a fluorescent stereomicroscope of injured mouse brains with no graft (**A**) or with transplants made of cortical-like derivatives generated from Bp-ESC (**B**) or Pg-ESC (**C**). Dashed lines show the presumptive injured cortical motor and visual areas. **D–I** are higher magnifications of **A–C**. The visual lesions of Bp (**F**) and Pg (**H**), and motor lesion of Pg (**I**) transplanted animals contained a transplant. **J–O.** Efficiency of Bp and Pg transplantation. Immunostainings against GFP were performed on free-floating sections. Examples illustrating the absence of graft (**J**, **M**) and the presence of GFP⁺ Bp (**K**, **N**) and Pg transplants (**L**, **O**). Scale bars: 1 mm. **P–U.** Cortical transplants express neural

markers. Immunostainings against TUBB3 (**P, S**), GFAP (**Q, T**), and POU3F2 (**R, U**) were performed on GFP⁺ cortical Bp and Pg transplants. Scale bars: 50 μm for P, Q, S, and T, and 20 μm for R and U.

Author Manuscript

Author Manuscript

Author Manuscript

Author Manuscript

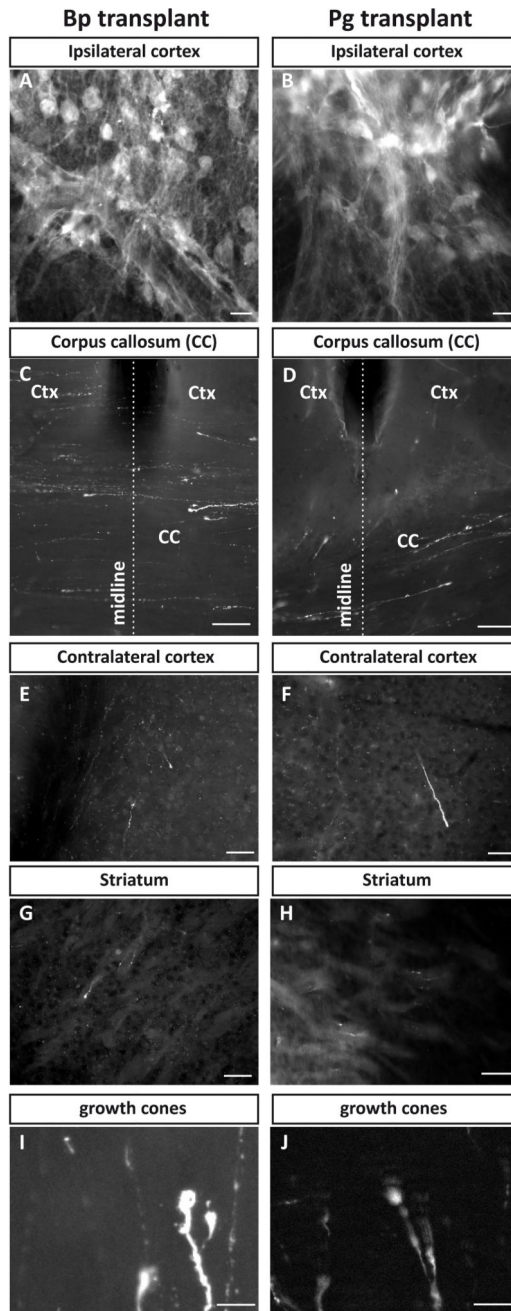


Fig. 7. Pg transplants send axonal projections that are typical of cortical neurons
 Both Bp and Pg transplants sent numerous GFP⁺ projections, in vicinity of the transplant (ipsilateral cortex –Ctx- (A, B), in the corpus callosum –CC- (C, D), in the contralateral cortex (E, F) and in the striatum (G, H). Some Bp and Pg axons ended by a growth cone-like protrusion (I, J). Scale bars: 20 μ m for A–B, 50 μ m for C–H and 10 μ m for I–J.